Identification of effective best management practices in sediment yield diminution using GeoWEPP: the Kasilian watershed case study

Amin Reza Meghdadi

Abstract Identifying areas that are susceptible to soil erosion is crucial for water resource planning and management efforts. Furthermore, modeling has proven helpful in recognizing and monitoring high-risk areas at the watershed scale. The Water Erosion Prediction Project (WEPP) geospatial interface (GeoWEPP) software integrates GIS with the WEPP to analyze the spatial variation in soil loss, and it has been used as a modeling tool to determine the areas that are most prone to soil erosion and to evaluate best management practices for the Kasilian watershed in Iran. As much as 62.4 % of the agronomic land in the Kasilian watershed is affected by a high magnitude of erosion (>5 t/ha). On the basis of this study, by using soybeans, high fertilization levels, and the drill-no-tillage system, reductions of erosion by almost 32.68–34.02 % are perceivable in three critical subwatersheds that are located in the cultivated lands. Also, it is projected that reductions in the production of sediment in the range of about 36.7–47.1 % are achievable by structural management within two critical, upland subwatersheds. So, by utilizing the best management strategies, sediment yield can be lowered and the conservation of soil and water is feasible at the watershed scale. These results objectively indicate that GeoWEPP can be efficaciously used for evaluating effective management practices for developing watershed conservation.

Introduction

Soil erosion is globally recognized as a significant environmental problem with major financial repercussions. In Iran, specifically, water- and wind-induced soil erosion is of major concern as it affects 62 Mha out of a total of 165 Mha (Saha 2003). To minimize soil loss, it is important to better understand the factors and areas that are most affected by soil loss. GIS-based spatial modeling has emerged as an important tool in soil erosion studies and consequently in the development of appropriate soil conservation strategies, especially at the watershed scale (Memarian et al. 2012). Modeling has formed the core of the research on the geographic aspects of the environment and has helped understand the distribution and spatial relations (Guillermo and Consuelo 2007). During the last three decades, researchers have developed hydrological models of empirical or conceptual nature for predicting hydrological variables, e.g., SWAT (Arnold et al. 1998), AGNPS (Young et al. 1989), ANSWERS (Beasley et al. 1980), and Water Erosion Prediction Project (WEPP; Laflen et al. 1991).

The WEPP is a physically based distributed model that predicts soil loss and deposition using a spatial and temporal distribution approach (Amore et al. 2004). The WEPP model is one of the most utilized tools for simulating water erosion and sediment yield

A. Reza Meghdadi (✉)
Department of Technical and Engineering, Science and Research Branch, Islamic Azad University, Tehran, Islamic Republic of Iran
e-mail: Ameghdadi5@gmail.com

(Sy). The model has been widely applied to predict runoff and Sy at the field and watershed scale (Nearing et al. 1989; Flanagan and Nearing 1995; Savabi et al. 1995; Brazier et al. 2000; Roswell 2001; de Jong van Lier et al. 2005). Integration of WEPP with geographic information systems (GIS) is desirable because it facilitates and improves the application of the model. WEPP geospatial interface (GeoWEPP) is a geospatial erosion prediction model with an ArcGIS interface that overcomes the limitations of WEPP, which are the manual input of the data and its application to small watersheds.

In this study, we input data for year 2000 to obtain WEPP output data that we subsequently used in the GeoWEPP model to recognize and predict areas with the greatest Sy in the Kasilian watershed. This is the first time that the GeoWEPP model has been used in such a manner in Iran, and it adds to previous studies (Solaimani and Darvari 2008; Gholami et al. 2009; Abadi and Ahmadi 2011). The Kasilian watershed is an area of forests and mountains that is part of the Caspian Sea watershed, the largest enclosed inland body of water on Earth, which has been adversely impacted by the destruction of forest lands, changes in land use, and impervious surface development (Gholami et al. 2009). At the present time, there is no Sy distribution map for the Kasilian watershed, and there are no sufficient data to monitor the areas that are most affected by the loss of soil and the accumulation of sediment, both of which are known as non-point-source pollution. In this watershed, about 25.7 % of all areas are eroded twice per year, during spring and autumn. Furthermore, we have applied crop and tillage management to reduce the amount of sediment in agronomic subwatersheds, and we also have used structural management for the same purpose in hilly subwatersheds. Also, we tested the effectiveness of GeoWEPP for prioritizing and evaluating the best management practices.

Materials and methods

Study area

The Kasilian watershed is located between longitude 53°1′16″ to 53°8′35″ and latitude 36°4′1″ to 36°8′14″ (Fig. 1). The watershed covers an area of 68.3 km², and it is 17.11 km long and 3.98 km wide with a minimum and maximum altitude of 1,120 and 3,123 m above MSL.

The watershed is steep with an average slope of 24.2 % (13.6°). The minimum and maximum monthly temperatures vary from −14.5 to 37.5 °C. The daily mean relative humidity varies from a minimum of 24.3 % in March to a maximum of 55.7 % in August. The average precipitation from 2000 to 2009 was 1,050 mm and for 2000, which is of interest in this study, was 980 mm. Nearly 74 % of the total rainfall is received during June and October. The overall climate of the area can be classified as subhumid tropical. Bright sunshine varies from 9 to 14 h during the dry months and 5 to 9 h during the rainy months. Monthly mean wind speeds was the highest in April with an average value of 6.32 km/h and lowest in September with an average value of 1.36 km/h. Sand and silt are the dominant soil types, and limestone soils are sparse. 72.2 % of the watershed is covered by natural forests with dense to slightly moderate biomass. Agricultural land represents 20 % of the watershed and the remaining land use is pasture and residential areas.

Water erosion prediction project

The WEPP model is a distributed parameter, one-dimensional, process-based erosion model that is used to predict Sy and runoff volume during storm events by simulating the detachment, transport, and deposition of sediment on rectangular hill slopes during runoff events (Flanagan and Nearing 1995). The WEPP model requires four input files including slope, climate, soil, and management files that describe the hillslope geometry, meteorological characteristics, soil properties, and ground cover. It is a widely used model to predict soil erosion (Merritt et al. 2003), average runoff, and soil loss under different conditions (Bhuyana et al. 2002; Tiwari et al. 2000; Ghidey and Alberts 1996; Kramer and Alberts 1995).

The WEPP model uses the fundamentals of infiltration, surface runoff, plant growth, residue decomposition, hydraulics, tillage, management, soil consolidation, and erosion mechanics, including the estimation of the spatial and temporal distribution of net soil loss (Nearing et al. 1989). The model mainly uses physically based equations to describe hydrologic and sediment generation and transport processes at the hillslope and stream scale.

GeoWEPP description

The GeoWEPP combines GIS and WEPP and was collaboratively developed by the Agriculture Research Service, Purdue University, and the USDA National
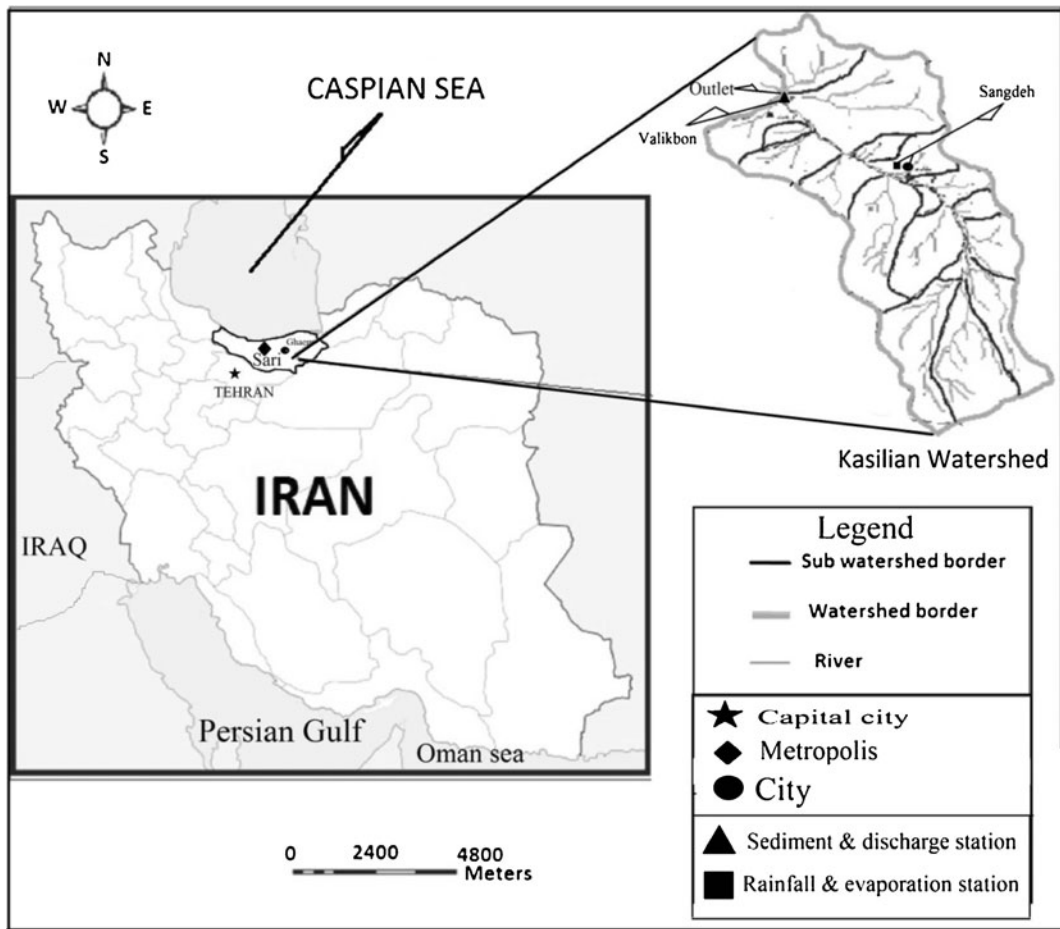
Fig. 1 Location map of the study area and subwatersheds

Soil Erosion Research Laboratory (Renschler and Harbor 2002). It consists of three parts: the GIS model, topography parameterization (TOPAZ), and Top WEPP. The program first establishes a digital elevation map (DEM), land use map, and soil distribution map using the spatial analysis function in ArcGIS 9 Then, it analyzes the DEM data by using TOPAZ with the aim of forming an accordant junction network in the watershed. Subsequently, it overlays the land use, or land management related to human activities, and soil maps to produce the basic unit of the watershed, which is the subwatershed (Yu et al. 2009).

TOPAZ determines the channel network based on the steepest down-slope path, considering eight adjacent cells for each raster cell (pixel) (Garbrecht and Martz 1997). The channel network can be adjusted by changing the values of the mean source channel length (MSCL) and critical source area (CSA). The MSCL defines the shortest

channel length, and CSA is the minimum drainage area (Yuksel et al. 2008). After defining the channel network, TOPAZ generates the subwatershed.

GeoWEPP input files

Climate

To generate the climate file with the daily values of precipitation, temperature, solar radiation, and wind speed obtained from the weather stations, the WEPP model uses CLIGEN, which is a stochastic weather-generation model. For a specific location and length of time, the Rock Clime application in the Forest Service WEPP is used to determine the spatial climate variability in mountain regions (Elliot et al. 1999). To generate the climate data, Rock Clime can access the Parameter Elevation Regressions on Independent Slopes Model

database which estimates the precipitation and temperature based on orographic effects (Daly et al. 1994). In Rock Clime, the monthly average precipitation and temperature input values can be adjusted (Elliot et al. 1999). Since the meteorological database in Iran is not generated in the data format of the CLIGEN model, the climate parameters for the study area were obtained from the Sangdeh and Valikben weather stations (Fig. 2a), and subsequently transformed into the format used in CLIGEN. The input climate parameters are the maximum and minimum air temperature, relative humidity, precipitation, solar radiation, and wind speed.

Slope

The drainage network and elevation contours at 20-m intervals were digitized using the Arc-Info GIS software and a survey of the Kasilian 1:25,000 scale top sheets. The digitized contours were used to generate a digital elevation model with a grid cell resolution of 50 m (Kienzle 1996; Renschler et al. 1997). Furthermore, the DEM was used to generate the slope aspect and slope shape factor grids for the study area (Fig. 2b).

Management

The default crop parameter values contain three parts. The first part depends on the management exerted on the watershed, the second part on the initial conditions, and the third part is the physiological characteristics of plants. The forest specifications for the input management file were extracted from the WEPP default database (type 1, perennial forest; type 2, 5-year perennial forest; type 3, residual areas; type 4, pasture; and type 5, agricultural (corn and alfalfa)) (Fig. 2c). Plant specification parameters for corn and alfalfa (conventional crops in watershed) are adopted from WEPP default database at average productivity level and also from Ascough et al. (1995). Model input parameters for corn and alfalfa for Kasilian condition are presented in Tables 1 and 2, respectively. The amount of ground cover is indicated in the management file based on growth and mortality parameters. WEPP generates inter-rill cover data for each year using growth parameters, soil data, and climate data. To generate the desired amount of ground cover in each site, each year, WEPP adjusts the biomass energy ratio in the management file.

Soil

The interface makes use of digital soil maps in which the different polygons represent different soil units. The maps are related to two databases describing the physical and chemical characteristics of the different horizons in the soil profile. For the present case study, a high-resolution, digital 1:25,000 soil map published by the Sari Natural Resources Organization was used (Fig. 2d). It classifies the soil by functional horizons according to the evaluated soil profiles, which is highly suitable to modeling.

Results and discussion

In the present study, the calibration procedure was conducted manually based on trial and error (Sorooshian and Gupta 1995) for the year 2000. Sensitivity analysis of the model was scrutinized based on the soil-related parameters by varying one parameter and keeping the others constant. The soil-related parameters that were scrutinized for sensitivity analysis were interrill erodibility (K_i), rill erodibility (K_r), effective hydraulic conductivity (K_e), and critical hydraulic shear stress (τ_c). The effects of these parameters on the response of the model response are shown in Table 3 by changing ±50 % from the calibrated value. The values of the parameters were selected within the recommended values proposed by Flanagan and Livingston (1995), and, according to the methods suggested by Xevi et al. (1997), several simulations were conducted by modifying the values of the parameters until the minimum quantity for root mean square error (RMSE) and the maximum quantity for the model-fit efficiency coefficient of the Nash and Sutcliffe (NSE) were acquired.

Daily values of simulated runoff and Sy in 2000 were compared graphically with measured values, and the results are shown in Figs. 3 and 4, respectively. (Daily rainfalls that were less than 5 mm were ignored because of their negligible influence on the production of sediment). Runoff and sediment data at the outlet of the watershed during 2000 were collected by Sari Natural Resources Organization as described below:

> Daily runoff volume—obtained by using a water stage level recorder with a rectangular weir.
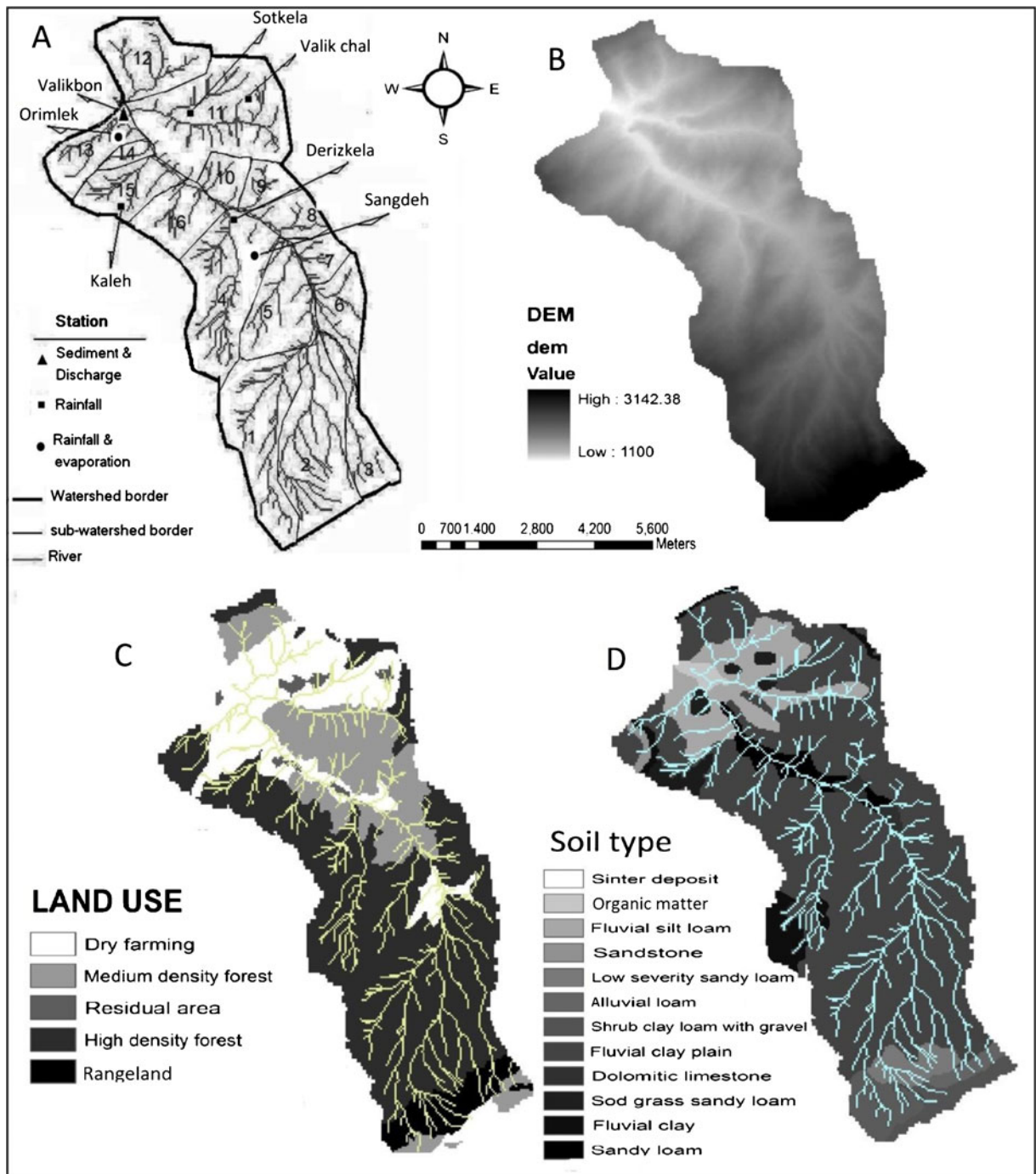
Fig. 2 **a** Location of the rain gage stations and the 16 subwatersheds in the Kasilian watershed; **b** digital elevation model map; **c** land-use map; and **d** soil-type map

Flow velocity—obtained by using a current meter (for all rainfall events).

Sediment flow—measured for each storm manually by using a USDH-48 bottle silt sampler.

According to Table 3, the most sensitive parameter that affects the yield of runoff is K_e, and the most sensitive parameters that affect the yield of sediment are K_e and K_i. These factors reveal the dominancy of

Table 1 Model input parameters for corn

Input variable	Value	Comments
Canopy cover coefficient	3.8	Ascough et al. (1995)
Parameter value for canopy height equation	3.1	Ascough et al. (1995)
Biomass energy ratio (kg/MJ)	35	Assumed
Base daily air temperature (°C)	20	Observed
Parameter for flat residue cover equation (m^2/kg)	2.3	Assumed
Growing degree days to emergence (°C days)	55	Assumed
Critical live biomass value below which grazing is not allowed (kg/m^2)	0	Assumed
Height of postharvest standing residue; cutting height (cm)	28.5	Observed
Percent canopy remaining after senescence (%)	76	Assumed
Plant stem diameter at maturity (cm)	3.9	Observed
Percent of growing season when leaf area index starts to decline (%)	90	Ascough et al. (1995)
Percent of biomass remaining after senescence (%)	89	Ascough et al. (1995)
Radiation extinction coefficient	0.7	Assumed
Standing to flat residue adjustment factor (wind, snow, etc.; %)	99	Ascough et al. (1995)
Maximum Darcy–Weisbach friction factor for living plant	1.1	Estimated
Growing degree days for growing season (°C days)	1700	Assumed
Harvest index (dry crop yield/total above ground dry biomass; %)	50	Observed
Maximum canopy height (cm)	215	Ascough et al. (1995)
Use fragile or nonfragile mfo values	N–fragile	Assumed
Decomposition constant to calculate mass change of aboveground biomass	0.0065	Assumed
Decomposition constant to calculate mass change of root biomass	0.0065	Assumed
Optimal temperature for plant growth (°C)	25	Observed
Plant specific drought tolerance (% of soil porosity; %)	25	Ascough et al. (1995)
In-row plant spacing (cm)	21.9	Assumed
Maximum root mass for a perennial crop (kg/m^2)	0	Assumed
Period over which senescence occurs (days)	29	Ascough et al. (1995)
Maximum temperature that stops the growth of a perennial crop (°C)	0	Estimated
Critical freezing temperature for a perennial crop (°C)	0	Estimated
Maximum leaf area index	3.5	Assumed

interrill erosion in the soil erosion process and of the conductivity of the water in surface soil in generating runoff. Comparable and commensurate results have been described in previous studies (Bhuyana et al. 2002; Pandey et al. 2008; Singh et al. 2011); therefore, more accurate assessment for these parameters was required.

The coefficient of determination (R^2), RMSE, and the model-fit efficiency coefficient, of NSE (ASCE Task Committee 1993) were used to assess the accuracy of the GeoWEPP software in predicting runoff and Sy in the Kasilian watershed. The close correlation between the values of observed and simulated runoff and Sy was demonstrated for the calibration

period (2000). As shown in Table 4, NSE=0.82 and RMSE=0.01549 in the prediction of Sy indicated very good agreement between output of the model and the observed values. Runoff has a significant effect on sediment generation and transport, so it is crucial to simulate runoff in order to achieve the accurate simulation of Sy for use in attaining precise, practical, and effective watershed management.

Spatial distribution map of Sy

In the present study, we used input data for the year 2000 to establish and predict Sy in the Kasilian watershed. After running the GeoWEPP model, the Sy

Table 2 Model input parameters for alfalfa

| Input variable	Value	Comments
Canopy cover coefficient	15	Ascough et al. (1995)
Parameter value for canopy height equation	23	Ascough et al. (1995)
Biomass energy ratio (kg/MJ)	13	Ascough et al. (1995)
Base daily air temperature (°C)	6	Observed
Parameter for flat residue cover equation (m^2/kg)	5	Assumed
Growing degree days to emergence (°C days)	30	Assumed
Critical live biomass value below which grazing is not allowed (kg/m^2)	0.1	Assumed
Height of postharvest standing residue; cutting height (cm)	17	Observed
Percent canopy remaining after senescence (%)	90	Assumed
Plant stem diameter at maturity (cm)	0.53	Observed
Percent of growing season when leaf area index starts to decline (%)	80	Ascough et al. (1995)
Percent of biomass remaining after senescence (%)	88	Ascough et al. (1995)
Radiation extinction coefficient	0.55	Assumed
Standing to flat residue adjustment factor (wind, snow, etc.; %)	89	Ascough et al. (1995)
Maximum Darcy–Weisbach friction factor for living plant	14.5	Estimated
Growing degree days for growing season (°C days)	0	Assumed
Harvest index (dry crop yield/total above ground dry biomass; %)	80	Observed
Maximum canopy height (cm)	75	Ascough et al. (1995)
Use fragile or non-fragile mfo values	Fragile	Assumed
Decomposition constant to calculate mass change of aboveground biomass	0.015	Assumed
Decomposition constant to calculate mass change of root biomass	20	Assumed
Optimal temperature for plant growth (°C)	22	Observed
Plant specific drought tolerance (% of soil porosity; %)	0.55	Ascough et al. (1995)
In-row plant spacing (cm)	240	Assumed
Maximum root mass for a perennial crop (kg/m^2)	0.6	Assumed
Period over which senescence occurs (days)	12	Ascough et al. (1995)
Maximum temperature that stops the growth of a perennial crop (°C)	28.5	Estimated
Critical freezing temperature for a perennial crop (°C)	0.49	Estimated
Maximum leaf area index	6	Assumed

distribution map was derived to visualize the spatial distribution of Sy and identify the areas that are most susceptible to erosion (Fig. 5).

The Sy map produced by the model for the Kasilian watershed is shown in Fig. 5. Land area, land use, soil type, and Sy rates are listed in Table 5. The flattest

Table 3 Sensitivity analysis of the model

Output value	Sensitive parameters	Calibrated value	Percent change in output value (%)	
			−50	+50
Runoff	K_e (mm h^{-1})	10.78	11.29	−6.86
	K_e (mm h^{-1})	10.78	8.2	−7.12
Sediment yield	K_i (kg s^{-1} m^{-4})	190,200	−3.73	8.28
	K_r (s m^{-1})	11.2*10^{-3}	−4.44	3.11
	τ_c (N m^{-1})	6.32	−3.7	4.32

Fig. 3 Comparison between the daily and observed and simulated runoff for the year 2000
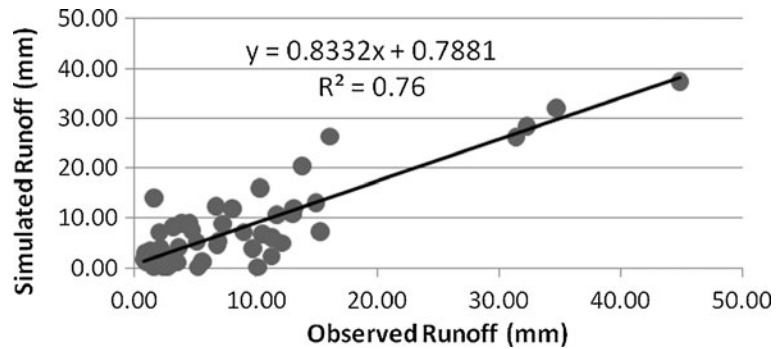
parts of the watershed had low yields of sediment (0–0.25 t/ha). In the central part of the watershed, the dominant perennial forest apparently maintained the sediment rate at 0.25–0.75 t/ha irrespective of the slope. The highest Sy (>4 t/ha) occurred in the highest altitude areas where the slope angle exceeded 40°. Although it seemed that the model predicted high rates of Sy in the high-slope areas, a different picture emerged when the histogram of the quantification of the pixels was constructed.

The land in the southern heights of the Kasilian watershed is pasture with sandy loam soil and a mean slope angle greater than 40°. Low-severity soil burns and the steepness of the high slopes are the major contributors to the high Sy (>4 t/ha) in this area. Moreover, in the northern parts of the watershed, the mean slope angle is less than 15°. In the flatter areas, most of the sediment load settles down because of gravity.

The analysis gives an overview of the off-site erosion damage and covers in detail the spatial and temporal aspects of erosion. The average model sediment rate for the total cultivatable lands was 1.88 t ha^{-1} year^{-1}. In

about 20.9 % of the watershed, the sediment rate produced by the model was greater than 4 t ha^{-1} year^{-1}, and consequently, the soil erosion risk is greater. It also is noteworthy that the large rills in the Kasilian watershed accounted for more than 24.5 % of the total loss of soil.

Identification and prioritization of critical subwatersheds

In the present study, annual Sy for all subwatersheds of the study area in the year 2000 were estimated (Table 6). Figure 4 shows that the simulated Sy was in close agreement with the measured yield, and it is convenient and appropriate to use the output of the model (in the absence of measured data for the outlet of each subwatershed) for identification and prioritization of critical subwatersheds in the Kasilian watershed. According to Table 6, the sediment load varied from a low of 0.5 t/ha to a high of 5.8 t/ha in subwatersheds 9 and 11, respectively. Five out of the 16 watersheds, i.e., No. 1, 2, 11, 12, and 15 (Table 6), were the most susceptible to the generation of sediment.

Fig. 4 Comparison between the daily observed and simulated Sy for the year 2000
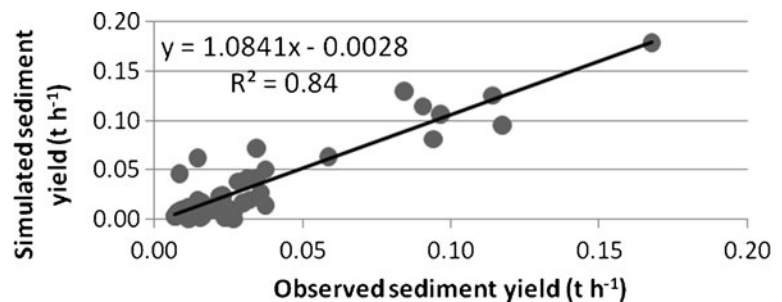
Table 4 Goodness of fit statistics of measured and simulated daily runoff and sediment yield

Statistical parameter	Runoff (mm)		Sediment yield (th⁻¹)	
	Observed	Simulated	Observed	Simulated
Mean	8.20	7.615	0.0314	0.0312
STDEV	9.1269	8.6932	0.0333	0.0392
Max	44.85	37.33	0.17	0.18
Total	443.06	411.14	1.7	1.69
N	54	54	54	54
RMSE	4.466		0.01549	
NSE	0.75		0.83	
Rsq	0.76		0.84	

In the No. 1 subwatershed, the high-average slope and low-severity soil burns contributed to the high Sy (Table 6).

Subwatershed No. 2 is located in the steepest part of the Kasilian watershed, and the average slope exceeds 68° (Table 6) and the high-severity soil burns and high
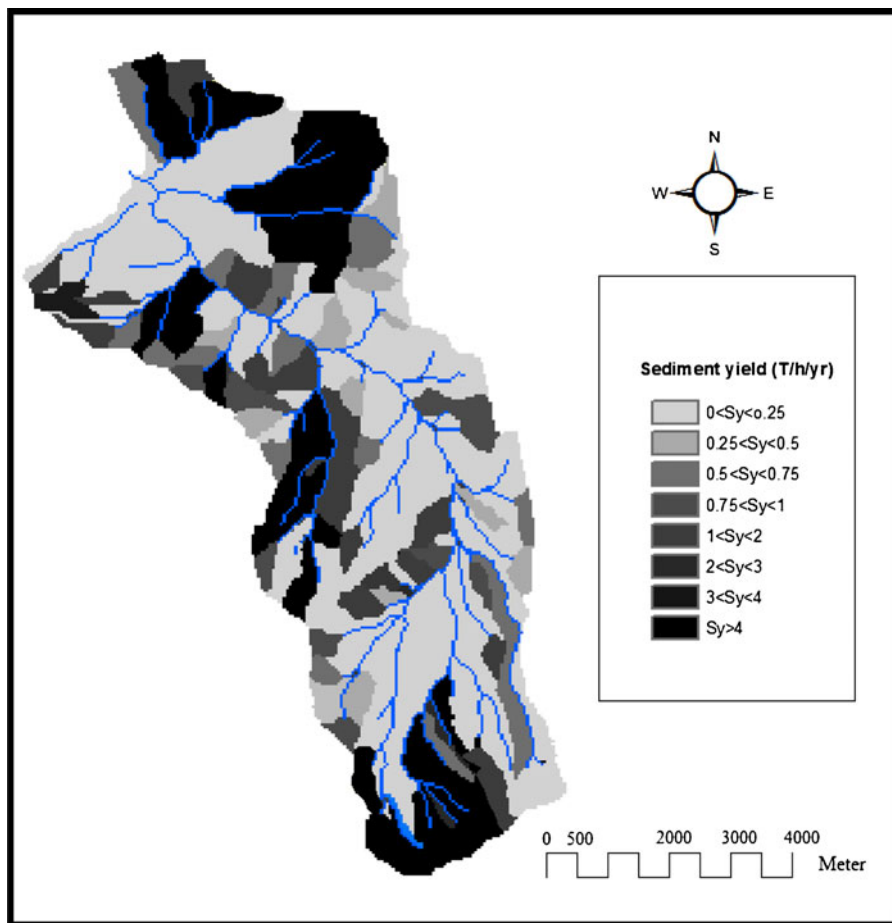

Fig. 5 Model soil loss distribution map of the Kasilian watershed based on input data from the year 2000

Table 5 Land area and use, slope, soil type, and corresponding soil loss rate

Sediment yield (yearly rate) (t/ha^{-1}/ year^{-1})	Area (%)	Slope (%)	Soil type (dominant)	Land use (dominant)
0–0.25	10.6	8	Sinter deposit and fluvial silt loam	Dry farming and medium-density forest
0.25–0.5	4.5	6	Shrub clay loam and organic matter	Medium-density forest
0.5–0.75	2.2	4	Sod grass sandy loam	Medium-density forest
0.75–1	37.5	13	Sandy loam	Dry farming
1–2	20.5	15	Sandstone	High-density forest
2–3	2.0	18	Sandy loam	High-density forest
3–4	1.6	14	Dolomitic limestone and sod grass sandy loam	Dry farming
>4	20.9	26	Alluvial loam, low-severity burn sandy loam, and fluvial silt loam	Dry farming and rangeland

slopes contribute to the high Sy. In subwatersheds No. 11 and 12, the average slope is less than 8 % (Table 6); however, they exhibit the greatest Sy with low-severity soil burns (Table 5) being the most dominant factor in the generation of sediment. However, there are several subwatersheds in which higher values of Sy were observed, and these may correspond to the unprotected areas that normally are located on the steepest slopes facing rivers or located in agricultural areas that require soil conservation.

Sy values greater than 5 t/ha were observed in 44 and 52 % of subwatersheds No. 11 and 12, respectively. Furthermore, more than 75 % of the agricultural land lies in these two subwatersheds. Thus, approximately 62 % of the total arable farmland in the Kasilian watershed is affected by erosion. The No. 4 subwatershed is located in the western part of the Kasilian watershed where there are high-density forests, and about 33.4 % of this subwatershed (about 2.74 km^2) had a high yield of sediment. In this area, there are sandy loam and

Table 6 Sub-watershed area and soil type and sediment yield

Subwatershed No.	Area (km^2)	Soil type	Sediment yield (t/ha)	Average slope (%)	Rank11
1	8	Low-severity burn sandy loam	4.8	41	3
2	9.0	Shrub clay loam with gravel	3.6	68.3	5
3	3.2	Shrub clay loam with gravel	1.71	27.1	10
4	8.1	Sandy loam and fluvial clay	3.4	24.0	6
5	4.9	Shrub clay loam with gravel	1	17.8	13
6	3.1	Shrub clay loam with gravel	1.7	10.0	11
7	1.5	Shrub clay loam and dolomitic limestone	2	17.5	8
8	2.5	Shrub clay loam and dolomitic limestone	0.9	15.8	14
9	1.5	Shrub clay loam with gravel and organic	0.45	17.6	16
10	1.8	Fluvial silt loam	1.4	17.9	12
11	10.3	Fluvial silt loam	5.8	8.0	1
12	5.2	Fluvial silt loam	5.2	6.4	2
13	3.3	Fluvial silt loam and shrub clay loam	1.8	28.0	9
14	0.8	Fluvial clay	2.1	20	7
15	4.9	Sod grass sandy loam	3.9	14.3	4
16	3.8	Fluvial clay plain	0.5	9.2	15

fluvial clay soils, which probably are responsible for the high yield of sediment.

Effective management of critical subwatersheds

Two critical districts in the watershed were identified to evaluate effective management strategies: (1) the southern height of the watershed (subwatersheds No. 1 and 2) with high-density forest and perennial land use and (2) the northern flat lowland (subwatersheds No. 11, 12, and 15) with agronomic land use and corn, low fertilization level, and mould board plough management. Therefore, efficient management practices are required in order to reduce Sy in these two critical districts.

Cultivated land

Efforts were made to reduce Sy and nutrient losses to evaluate the effectiveness of various management strategies by simulating crops viz., peanuts, sorghum, and soybeans at three fertilization levels (low, medium, and high) for No. 11, 12, and 15 subwatersheds. The results are presented in Table 7.

As shown in Table 7, when peanuts and soybeans were cultivated in subwatershed No. 15, Sy were reduced by about 12.3 and 18.13 %, respectively. When

Table 7 Effect of fertilization level and specific crops on sediment yield from critical subwatersheds

Treatment	Change in sediment yield in critical subwatersheds (%)		
	11	12	15
C1	+12.31	+13.23	+15.51
C2	+8.56	+10.11	+11.73
C3	+3.32	+5.72	+9.23
C4	−0.97	−1.01	−2.01
C5	−4.8	−7.14	−8.22
C6	−11.81	−11.38	−12.31
C7	−8.3	−7.15	−3.11
C8	−12.11	−11.12	−12.18
C9	−13.32	−11.21	−18.13

"+" increase, "−"decrease, *C1* sorghum (LFL), *C2* sorghum (MFL), *C3* sorghum (HFL), *C4* pea nut (LFL), *C5* pea nut (MFL), *C6* pea nut (HFL), *C7* soybean (LFL), *C8* soybean (MFL), *C9* soybean (HFL)

Table 8 Effect of tillage treatment on sediment yield from critical subwatersheds

Treatment	Change in sediment yield in critical subwatersheds (%)		
	11	12	15
TI	−9.34	−8.22	−6.15
TII	−16.68	−15.56	−12.87
TIII	+19.36	+17.49	+14.32
TIV	−15.44	−14.97	−10.36

"+" increase, "−"decrease, *TI* field cultivator, *TII* drill no tillage, *TIII* harrow spike tooth, *TIV* drill single disk opener

these same two crops were grown in subwatershed No. 11 (major priority), Sy were reduced by about 11.8 and 13.2 %, respectively. Thus, it can be inferred from Table 7 that Sy can be reduced by substituting cash crops, such as peanuts and soybeans, for corn. Corn is the staple food for the people of the watershed, so reasonable efforts should be expended to replace this prior crop in these subwatersheds, to improve the economy of the local people, reduce the sediment load, and increase nitrogen fixation in the soil. Reduction in sediment load for high fertilization levels (HFL) may be a consequence of the intensification of the density of plants, which increases the canopy cover and the roughness of the surface soil.

The effects of tillage treatments on Sy for the customary crop were used to simulate the results, and their influences are shown in Table 8 for four tillage treatments viz., field cultivation, a drill-no-tillage system, harrow spike tooth, and drill single disk opener. These four treatments were considered as replacements for

Table 9 Effective management strategies for reducing sediment yield

Change in sediment yield in critical sub watersheds (%)			
Management practices	11	12	15
MP1	−26.39	−25.10	−22.11
MP2	−30.33	−28.06	−24.59
MP3	−31.42	−28.62	−31.26
MP4	−32.68	−29.35	−34.02

"−"decrease, *MP1* pea nut (HFL, drill single disk opener), *MP2* pea nut (HFL, drill no tillage), *MP3* soybean (HFL, single disk opener), *MP4* soybean (HFL, drill no tillage)

Table 10 Simulated sediment yield budget in hilly critical subwatersheds for the year 2000

Subwatershed	Soil eroded from hillslopes (ton)	Soil deposited in hillslopes (ton)	Soil eroded from channels (ton)	Soil deposited in channels (ton)	Sediment yield at the out let (ton)
1	3,889.96	648.34	598.68	0	3,840. 3
2	3,299.19	546.18	487.22	0	3,240.23

conventional treatment (mould board plough) to provide advantageous and profitable treatment.

According to Table 8, various magnitudes of sediment reduction were evident in the critical subwatersheds when they were compared to the farmers' practice of mould board plough tillage. Maximum reduction in Sy occurred for the case of the drill-no-tillage system, followed by drill single disk opener. Due to the drainage density and steep topography of these major-priority subwatersheds, utilizing effective tillage treatment (TI and TIV) led to increased roughness of the surface soil, and extra depressions were attainable, causing excess infiltration and minor runoff productivity that redounded to minimum Sy.

The combination of efficient crop and tillage practices may lead to even greater reductions in Sy. So, as shown in Table 7, peanuts, HFL, and soybeans, HFL, have the highest efficacy for reducing Sy in these three critical subwatersheds. The same is true of drill single disk opener and the drill-no-tillage system in Table 8. So, these practices can be integrated to achieve the best management strategies for reducing Sy (Table 9).

As shown in Table 9, there were no significant differences among the various management practices. But the combination of soybeans, HFLs, and the drill-no-tillage system had the greatest impact on reducing the sediment, as did and soybeans, HFLs, and single-disk opener. Corn is grown in lowland, mildly sloped areas of the watershed, and it is the staple food for the

local people. This crop is profitable using any of the mentioned management practices (Table 9), so it is understandable that the farmers might resist replacing corn with other cash crops, such as soybeans and peanuts, for the purpose of reducing the sediment load and achieving better soil conservation.

Upland

Subwatersheds No. 1 and 2 are located in southern height of the Kasilian watershed with forests and perennial land uses and pastures. Using crop and tillage management is prohibited in this section because of the conservation strategies from Sari Natural Resources Organization. However, utilizing structural management is admissible in order to control sediment transport by channels in these areas.

The model-simulated sediment budget for 2000 in critical subwatersheds No. 1 and 2 is presented in Table 10.

It was concluded that between 15.58 and 15.03 % of total Sy was contributed by channel erosion; therefore, the sediment load can be controlled by depositing eroded soil from hillsides and also by controlling channel erosion by using structural impoundments.

From regional investigations and contemplating the availability and expenditure of local material, it was considered that there was only a slight chance of failure in the two types of impoundment structures, i.e., filter fence and check dam (Flanagan and Livingston 1995).

According to the dimensions of the channels (measured at the considered location) and default flow direction of the model, the database associated with this structure, which is located at the downstream side of a critical hillslope and contribute high Sy.

Simulation results (Table 11) indicated that the installation of 26 structures resulted in about 36.7 and 47.1 % reduction in sediment load in subwatersheds No. 1 and 2, respectively. The filter fence and check dam do not

Table 11 Effect of the filter fence and check dam on the reduction of sediment yield in two critical, hilly, subwatersheds from the year 2000

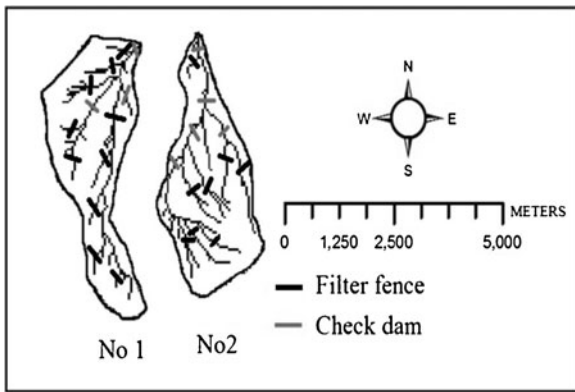| Subwatershed	Number—filter fence	Number—check dam	Percent change
1	10	3	−36.78
2	8	5	−47.11

Fig. 6 Location map of proposed structures in subwatersheds No. 1 and 2

block the flow movement completely. These low-cost structures reduce sediment in the channel, resulting in intensified sediment deposition and infiltration. The location map of these structures is shown in Fig. 6.

Effective management practices consequence on daily Sy

The four most effective management practices in reducing Sy in the year 2000 were considered (Table 9), and their efficacy in reducing the individual, daily, Sy based on model simulation at the watershed outlet is shown in Fig. 7.
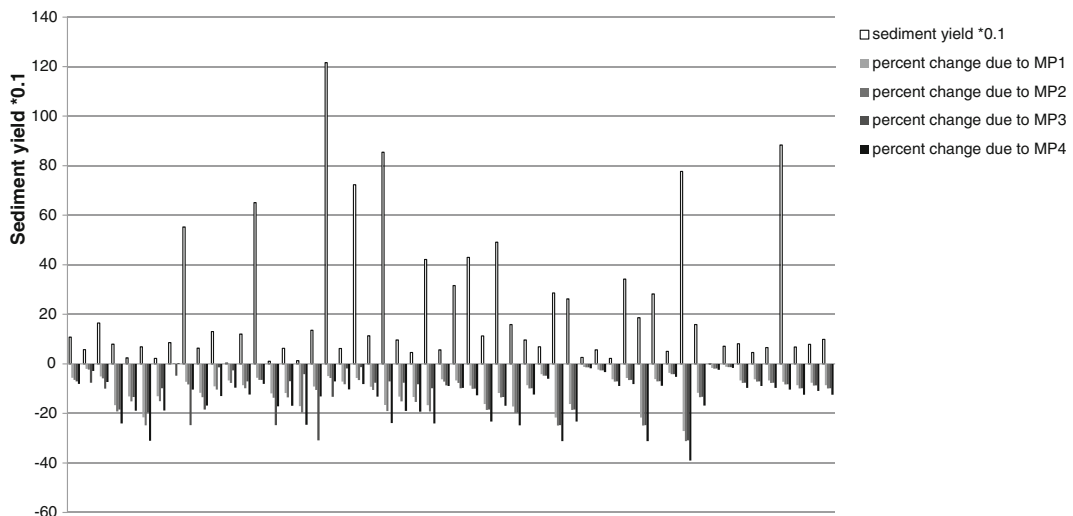
The greatest reduction in Sy is perceivable in MP4 practices. Also saturation level of the surface soil is intensified by small rainfall events that follow intense rainfall events and, as a consequence of the decrease in infiltration, runoff increases and causes the formation of high Sy. So, by utilizing best management practices, it is concluded that high percentages of reduction can be achieved. An increase in tillage depth from 20 to 40 cm can increase soil displacement by 75 % (St. Gerontidis et al. 2001) in high rainfall areas, and the mould board plough treatment (conventional treatment) may facilitate the formation of rills and may result in an increased erosion rate. Therefore, by using drill single disk opener and the drill-no-tillage system as tillage treatments for critical subwatersheds, and, as a result of the decreased tillage depth, dramatic reductions in Sy from the watershed outlet can be achieved in high rainfall areas.

Conclusions

We input WEPP model output data into GeoWEPP software and generated a Sy map for the Kasilian watershed to visualize soil erosion relative to elevation, land use, and soil type. We identified that the most susceptible areas to the loss of soil were the steepest slopes within the watershed. Although the map does not give the total Sy at the watershed level,

Fig. 7 Effect of effective management practices on daily Sy from the watershed outlet

it can be used to identify the areas that are the most susceptible to erosion.

It was inferred that the highest Sy comes from three subwatersheds, i.e., No. 11, 12, and 15, in the northeast part of the Kasilian watershed. In subwatersheds No. 11 and 12 that have an average slope of less than 8 % and low-severity soil burns, the Sy was more than 5 t/ha; therefore, the type of soil probably contributes more to the Sy process and the need for more effective management practices is apparent when we consider that more than 50 % of the cultivated land and more than 60 % of the agricultural land are located in these two subwatersheds. So, Sy were reduced in these three critical subwatersheds by approximately 28.2 to 34.02 % by applying MP1 and MP2 management practices.

Two subwatersheds, i.e., No. 1 and 2, had the highest Sy. Furthermore, the Sy in subwatershed No. 1 was 4.8 t/ha with an average slope of 41 %, and the yield in No. 2 was 3.6 t/ha with an average slope of about 68 %. Thus, the slope is likely the major contributing factor to the Sy process in these subwatersheds. So the total simulated Sy in these two subwatersheds were reduced by approximately 36.7 and 47.11 %, respectively, as a consequence of 26 structural impounds.

The results of this paper indicated that GeoWEPP software can be used effectively as a modeling tool for selecting better and more effective management strategies in order to fulfill the need for sustainable environmental developments.

References

Abadi, L. Z., & Ahmadi, H. (2011). Comparison of EPM and geomorphology methods for erosion and sediment yield assessment in Kasilian Watershed, Mazandaran Province, Iran. *Desert, 16*, 103–109.

Amore, E., Modica, C., Nearing, M. A., & Santoro, V. C. (2004). Scale effect in USLE and WEPP application for soil erosion compution from three Sicilian basin. *Journal of Hydrology, 293*(1–4), 100–114.

Arnold, G. J., Srinivasan, R., Muttiah, R. S., & Williams, J. R. (1998). Large area hydrologic modeling and assessment Part I: Model development. *Journal of the American Water Resource Association, 34*(1), 73–89.

ASCE Task Committee. (1993). Criteria for evaluation of watershed models. *Journal of Irrigation and Drainage Engineering, 119*(3), 429–442.

Ascough, J. C., Baffaut, C., Nearing, M. A., & Flanagan, D. C. (1995). Watershed model channel hydrology and erosion processes. In D. C. Flanagan & M. A. Nearing (Eds.), *USDA-water erosion prediction project hillslope profile and watershed model documentation* (pp. 117–137). West Lafayette: NSERL.

Beasley, D.B., Huggins, L.F., Monke, E.J. (1980). ANSWERS: A model for watershed planning. *Transactions of the ASAE, 23*(4), 938–944.

Bhuyana, S. J., Kalita, P. K., Janssenc, K. A., & Barnesa, P. L. (2002). Soil loss predictions with three erosion simulation models. *Environmental Modeling and Software, 17*(2), 135–144.

Brazier, R. E., Beven, K. J., Freer, J., & Rowan, J. S. (2000). Equifinality and uncertainty in physically based soil erosion models: application of the glue methodology to WEPP—the water erosion prediction project for sites in UK and USA. *Earth Surface Processes and Landforms, 25*, 825–845.

Daly, C., Neilson, R. P., & Philips, D. L. (1994). A statistical-topographic model for mapping climatologically precipitation over mountainous terrain. *Journal of Applied Meteorology, 33*, 140–158.

De Jong Van Lier, Q., Sparovek, G., Flanagan, D. C., Bloem, E., & Schnug, E. (2005). Runoff mapping using WEPP erosion model and GIS tools. *Computer & Geosciences, 31*, 1270–1276.

Elliot, W.J., Hall, D.E., Scheele, D.L. (1999). FS WEPP: Forest Service Interfaces for the Water Erosion Prediction Project Compute Model. http://forest.moscowfsl.wsu.edu/fswepp/docs/fsweppdoc.html. Accessed 10 September 2006.

Flanagan, D.C., Livingston, S.J. (1995). USDA-Water Erosion Prediction Project-WEPP User Summary. NSREL Report No.11. West Lafayette: USDA-ARS National Soil Erosion Research Laboratory.

Flanagan, D. C., & Nearing, M. A. (1995). *USDA Water erosion Prediction Project: hillslope profile and Watershed model documentation. NSERL Report No. 10*. West Lafayette: USDA-ARS National Soil Erosion Research Laboratory.

Garbrecht, J., & Martz, L. W. (1997). *TOPAZ: an automated digital landscape analysis tool for topographic evaluation, drainage identification, watershed segmentation, and sub catchment parameterization: overview ARS-NAWQL 95-1*. Durant: USDA-ARS National Soil Erosion Research Laboratory.

Ghidey, F., & Alberts, E. E. (1996). Comparison of measured and predicted runoff and soil loss for Midwest clay plain soil. *Transaction of the ASAE, 39*(4), 1395–1402.

Gholami, V., Jokar, E., Azodi, M., Zabardast, H. A., & Bashirgonbad, M. (2009). The influence of anthropogenic activities on intensifying runoff generation and flood hazard in Kasilian watershed. *Journal of Applied Sciences, 9*, 3723–3730.

Guillermo, A. B., & Consuelo, C. R. (2007). Assessment of erosion hotspot in watershed: integrating the WEPP model and GIS in case study in Peruvian Andes. *Environmental Modeling & Software, 22*(3), 1175–1183.

Kienzle, SW. (1996). Application of geographic information systems in hydrology and water resources management. In: Kovar, K, Nachtnebel, HP (Eds.). (pp 183–190). No. 235. Wallingford: IAHS-AISH Publication.

Kramer, L. A., & Alberts, E. E. (1995). *Validation of WEPP 95.1 Daily Erosion Simulation. ASAE Paper No. 95-2384, St.* Joseph: ASAE Publication.

Laflen, J. M., Lane, J. L., & Foster, G. R. (1991). WEPP—a new generation of erosion prediction technology. *Journal of Soil and Water Conservation, 46*(1), 34–38.

Memarian, H., Siva, K., Balasundram, S. K., Talib, J., Teh Boon Sung, C., Mohd Sood, A., et al. (2012). Hydrologic analysis of a tropical watershed using KINEROS2. *Environment Asia, 5*(1), 84–93.

Merritt, W. S., Letcher, R., & Jakeman, A. J. (2003). A review of erosion and sediment transport model. *Australian Journal of Soil Research, 39*, 1131–1145.

Nearing, M. A., Foster, G. R., Lane, L. J., & Finkner, S. C. (1989). A process-based soil erosion model for USDA-watershed erosion prediction project technology. *Transactions of ASAE, 32*, 1587–1593.

Pandey, A., Chowdary, V. M., Mal, B. C., Billib, M. (2008). Runoff and sediment yield modelling from a small agricultural watershed in India using the WEPP model. *Journal of Hydrology, 348*, 305–319.

Renschler, C. S., & Harbor, J. (2002). Soil erosion assessment tools from point to regional scales—the role of geomorphologists in Land management research and implementation. *Geomorphology, 47*, 189–209.

Renschler, C., Diekkruger, B., & Mannaerts, C. (1997). Regionalization in surface runoff and soil erosion risk evaluation. *Regionalization of Hydrology, 254*, 233–241.

Roswell, C. J. (2001). Evaluation of WEPP for runoff and soil loss prediction in Gunnedah, NSW, Australia. *Australian Journal of Soil Research, 9*, 230–243.

Saha, S.K. (2003), *Water and wind induced soil erosion assessment and monitoring using remote sensing and GIS*. In: M.V.K. Sivakumar, P.S. Roy, K. Harmsen, and S.K. Saha (Eds.), Training Workshop Proceedings (pp. 315–330). Geneva: World Meteorological Organization

Savabi, M. R., Flanagan, D. C., Hebel, B., & Engel, B. A. (1995). Application of WEPP and GIS-GRASS to small watershed in Indiana. *Journal of Soil Water Conservation, 50*, 477–483.

Singh, R. K., Panda, R. K., Satapathy, K. K. (2011). Simulation of runoff and sediment yield from hilly Watershed in the eastern himaliya. India using WEPP model. *Journal of Hydrology, 405*, 261–276.

Solaimani, K., & Darvari, Z. (2008). Suitability of artificial neural netweok in daily flow forecasting. *Journal of Applied Sciences, 8*(17), 2949–2957.

Sorooshian, S., & Gupta, V. K. (1995). Model Calibration. In V. P. Singh (Ed.), *Computer models for watershed hydrology* (pp. 23–68). Highland Ranch: Water Resources Publications.

St Gerontidis, D. V., Kosmas, C., & Detsis, B. (2001). The effect of mouldboard plow on tillage erosion along hillslope. *Journal of Soil and Water Conservation, 56*, 147–152.

Tiwari, A. K., Risse, L. M., & Nearing, M. A. (2000). Evaluation of WEPP and its comparison with USLE and RUSLE. *Transaction of the ASAE, 43*(5), 1129–1135.

Xevi, E., Christiaens, K., Espinao, A., Sewnandan, W., Mallants, D., Sorensen, H., et al. (1997). Calibration, validation and sensitivity analysis of the MIKE-SHE model using the Neuenkirchen catchment as a case study. *Water Resource Management., 11*, 219–242.

Young, R. A., Onstad, C. A., Bosch, D. D., & Anderson, W. P. (1989). AGNPS: A Non-point source Pollution model for evaluating agricultural watersheds. *Journal of Soil and Water Conservation, 44*(2), 168–173.

Yu, B., Zhang, X., & Niu, L. (2009). Simulated multi-scale watershed runoff and sediment production base on GeoWEPP model. *International Journal of Sediment Research, 24*, 465–478.

Yuksel, A., Gundogan, R., Reis, M., & Cetiner, M. (2008). Application of GeoWEPP for determining sediment yield and runoff in Orcane creek watershed in Turkey. *Journal of Sensor Technology, 8*, 1222–1236.